Int J Infrared Milli Waves (2008) 29:499–507
DOI 10.1007/s10762-008-9346-9

# A Method for Removing the Effect of the Camera Radiance on the Infrared Image

**Shidu Dong · Xiaofan Yang · Wu Yang · He Yan · Yue Wang**

Received: 10 August 2007 / Accepted: 25 February 2008 /
Published online: 15 March 2008


**Abstract** The radiance coming from the interior of an uncooled infrared camera has significant effect on the quality of an infrared image. The classical two-point-correction (TPC) method fails to remove this effect where no TPC data is collected. To overcome this deficit, this paper presents a three-phase scheme. First, from a set of samples and through least squares fitting, how the TPC datum varies with the interior temperature of the camera is determined. On this basis, all the necessary TPC data are calculated. Finally, the collected infrared image is corrected with the TPC method. Theoretical analysis and experimental results show that, for a proper interior temperature of the camera, the scheme can remove the effect effectively.

**Keywords** Infrared image · Camera radiance · Two-point-correction · Least squares fitting

## 1 Introduction

Apart from the radiance coming from the object being focused, the pixels on the focal plane array (FPA) in a camera also receive the unfocused flux from the interior of the camera (*camera radiance* for short), which has significant effect on the quality of infrared image [1–3]. In addition, the camera radiance varies with the interior temperature of the camera (*camera temperature*), resulting from the change of the ambient temperature. Where the infrared images of the appointed high-temperature and low-temperature blackbodies (*two-point-correction data* or *TPC data*) can be acquired, the classical TPC method can effectively remove the effects of both the non-uniformity of the FPA and the camera radiance on the infrared image. Unfortunately, this method fails when the TPC data are unavailable.

S. Dong (✉) · X. Yang
College of Computer Science, Chongqing University, Chongqing 400044, China
e-mail: dongshidu@yahoo.com.cn

S. Dong · W. Yang · H. Yan · Y. Wang
Computer School, Chongqing Institute of Technology, Chongqing 400050, China

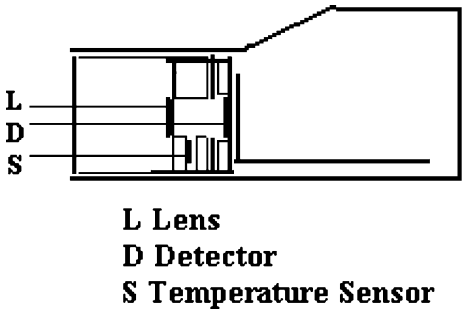


**Fig. 1** Illustration of an Infrared FPA camera.

To overcome the above mentioned deficit of the TPC method, this paper proposes a novel three-phase method, which is outlined below. First, from a set of samples and through least squares fitting, how each pixel value in the TPC data (*TPC datum*) varies with the camera temperature is determined. On this basis, all the necessary TPC data are calculated. Finally, the collected infrared image is corrected with the TPC method, and as a result, the effect is removed.

The paper is organized as follows: Section 2 provides the background knowledge and Section 3 indicates a shortcoming of the two-point-correction method. A new method for removing the effect of the camera radiance is proposed in Section 4. Experimental results are given in Section 5 and some conclusions are drawn in Section 6.

## 2 Background knowledge

Figure 1 plots an infrared focal plane arrays (FPA) camera. The detector used in the camera is an LW IRCMOS uncooled integrated microbolometer detector referenced as UL 01 01 1 made by ULIS [4] (see Fig. 2), which has 320×240 pixels and a spectral response ranging from 8 $\mu$m~14 $\mu$m.

The radiance reaching the camera can be modeled as:

$$E_B = \tau\varepsilon L_B(T_S) + \tau(1-\varepsilon)L_A(T_A) + (1-\tau)L_{ATM}(T_{ATM}), \tag{1}$$

where $L_B$ is the blackbody emittance, $\tau$ the atmosphere transmission coefficient, $\varepsilon$ the emissivity, $T_S$ the temperature of the object being focused, $T_A$ the ambient temperature of the object, and $T_{ATM}$ the atmospheric temperature [2, 5].

In what follows, we adopt the following two hypotheses.

(H1) The camera is close to the object, and $\tau$ is unity. This implies

$$E_B = \varepsilon L_B(T_S) + (1-\varepsilon)L_A(T_A). \tag{2}$$

**Fig. 2** UL 01 01 1 detector [4].

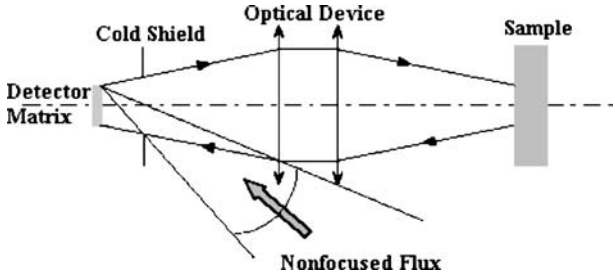


**Fig. 3** Radiance received by a pixel [1].

(H2) The object is a blackbody with emissivity $\varepsilon$=1. Then

$$E_B(T_B) = L_B(T_B) = L_B(T_S). \tag{3}$$

Despite a metal packaging is placed in front of the FPA, it can't remove the flux which doesn't come from the object via lens [1, 2] (see Figs. 2 and 3). Therefore pixels on FPA receive not only the radiance from the object being focused (*object radiance*), but also the camera radiance [1, 2, 6].

The radiance received by each pixel on the FPA, which is the sum of the blackbody radiance and the camera radiance, can be modeled as:

$$E_{i,j}(T_B, T_C) = \alpha^1_{i,j} E_B(T_B) + \alpha^2_{i,j} E_C(T_C), \tag{4}$$

where ($i$,$j$) denotes the position of the pixel on FPA, $T_B$ the blackbody temperature, $T_C$ the camera temperature, i.e. the readout of the temperature sensor $S$ (see Fig. 1), $E_C$ the camera radiance, and $\alpha_{i,j}{}^1$ and $\alpha_{i,j}{}^2$ constants. It should be indicated that the camera temperature varies with the ambient temperature. Indeed, experimental results show that the camera temperature is always higher than the ambient temperature.

Let $R_{i,j}$ denote the responsivity of the ($i$,$j$) pixel. Then, the intensity is determined by

$$\begin{aligned} D_{i,j}(T_B, T_C) &= R_{i,j} \times \left[\alpha^1_{i,j} E_B(T_B) + \alpha^2_{i,j} E_C(T_C)\right] + Off_{i,j} \\ &= R^1_{i,j} E_B(T_B) + R^2_{i,j} E_C(T_C) + Off_{i,j}, \end{aligned} \tag{5}$$

where $R^1_{i,j} = R_{i,j}\alpha^1_{i,j}$ denotes the responsivity of the ($i$,$j$) pixel to the object radiance, $R^2_{i,j} = R_{i,j}\alpha^2_{i,j}$ the responsivity to the camera radiance, and $Off_{i,j}$ a constant.

## 3 Shortcoming of TPC method

For each pixel on FPA, even though the value of $E_B(T_B)$ is constant, its pixel values is different because the values of $R^1_{i,j}$ and $R^2_{i,j}$ $E_C(T_C)$+$Off_{i,j}$ vary with the position ($i$,$j$) [7, 8]. To deal with this, the following equation, which is closely related to the two-point-correction (TPC) method [9], is often employed.

$$D'_{i,j}(T_B, T_C) = \frac{\overline{D}_H - \overline{D}_L}{D_{i,j}(T_H, T_{CR}) - D_{i,j}(T_L, T_{CR})} \times \left[D_{i,j}(T_B, T_C) - D_{i,j}(T_L, T_{CR})\right] + \overline{D}_L, \tag{6}$$

where $D_{i,j}(T_B,T_C)$ and $D'_{i,j}(T_B,T_C)$ are the original and corrected values of the $(i,j)$ pixel in the infrared image, respectively, $D_{i,j}(T_H,T_{CR})$ and $D_{i,j}(T_L,T_{CR})$ are the values of the $(i,j)$ pixels in the infrared images of the high-temperature and low-temperature blackbodies at the camera temperature $T_{CR}$, respectively, $D_H$ and $D_L$ are the mean values of $D_{i,j}(T_H,T_{CR})$ and $D_{i,j}(T_L,T_{CR})$, respectively, and $T_H$ and $T_L$ are the temperatures of the high-temperature and low-temperature blackbodies, respectively.

By Eq. 5, $D_{i,j}(T_L,T_{CR})$ and $D_{i,j}(T_H,T_{CR})$ can be written as

$$D_{i,j}(T_L, T_{CR}) = R^1_{i,j}E_B(T_L) + R^2_{i,j}E_C(T_{CR}) + Off_{i,j}, \tag{7}$$

$$D_{i,j}(T_H, T_{CR}) = R^1_{i,j}E_B(T_H) + R^2_{i,j}E_C(T_{CR}) + Off_{i,j}. \tag{8}$$

Substituting Eqs. 5, 7 and 8 into Eq. 6, we get:

$$D'_{i,j}(T_B, T_C) = \frac{\overline{D}_H - \overline{D}_L}{E_B(T_H) - E_B(T_L)} \times [E_B(T_B) - E_B(T_L)] + \frac{\overline{D}_H - \overline{D}_L}{R^1_{i,j}E_B(T_H) - R^1_{i,j}E_B(T_L)} \times \left[R^2_{i,j}E_C(T_C) - R^2_{i,j}E_C(T_{CR})\right] + \overline{D}_L \tag{9}$$

Let

$$Er_{i,j}(T_C, T_{CR}) = \frac{\overline{D}_H - \overline{D}_L}{R^1_{i,j}E_B(T_H) - R^1_{i,j}E_B(T_L)} \times \left[R^2_{i,j}E_C(T_C) - R^2_{i,j}E_C(T_{CR})\right]. \tag{10}$$

If the camera temperature $T_C$, where the infrared image is collected, is equal to that of the TPC data $T_{CR}$, then $Er_{i,j}(T_C,T_{CR}) = 0$. Thus,

$$D'_{i,j}(T_B, T_C) = \frac{\overline{D}_H - \overline{D}_L}{E_B(T_H) - E_B(T_L)} \times [E_B(T_B) - E_B(T_L)] + \overline{D}_L. \tag{11}$$

Equation 11 does not contain any item related to the camera radiance and the responsivity of the pixel. Therefore, when $T_C$ equals $T_{CR}$, TPC method can effectively remove the effects of the camera radiance and the non-uniformity of responsivity.

When $T_C \neq T_{CR}$, the TPC data at camera temperature $T_{CR}$ will be used to correct the infrared image collected at camera temperature $T_C$. In this case, an inspection of Eq. 10 concludes that $Er_{i,j}(T_C,T_{CR})$ is dependent on the camera radiance and the pixel responsivity. Furthermore, a larger difference between $T_C$ and $T_{CR}$ would yield a larger value of $Er_{i,j}(T_C,T_{CR})$ and hence a poorer quality of the corrected infrared image.

Therefore, the TPC method can remove the effect of the camera radiance only when the TPC data are available.

## 4 Proposed method

According to the above discussion, the TPC method doesn't effectively remove the effect of the camera radiance where no TPC data is available. Fortunately, through least squares fitting, the TPC data at any camera temperature can be worked out.

### 4.1 Fitting polynomial of the TPC data

From Eq. 5, the value of the $(i,j)$ pixel in the low-temperature blackbody image is governed by

$$D_{i,j}(T_L, T_C) = R^1_{i,j} E_B(T_L) + R^2_{i,j} E_C(T_C) + Off_{i,j}. \tag{12}$$

As $T_L$ is fixed, $R^1_{i,j} E_B(T_L)+Off_{i,j}$ keeps constant. As a result, $D_{i,j}(T_L,T_C)$ can be regarded as the function of $T_C$, which is often approximated by the following polynomial of degree $n$ [2, 10].

$$D_{i,j}(T_L, T_C) \approx F^n_{i,j}(T_C) = \sum_{k=0}^{n} a_k(i,j) T_C^k. \tag{13}$$

The values of $a_n(i,j),\ldots, a_0(i,j)$ can be determined by means of least squares fitting by using the $(i,j)$ pixel values in collected infrared images of the low-temperature blackbody at more than $n+1$ different camera temperatures (*training sample data*). In view of the working temperature range of the cameras from 278.15$K$ to 313.15$K$ (5°C to 40°C), which departs from origin, the normal equations of the fitting polynomial may be ill-conditional. To overcome the drawback, the following equation, a translation of Eq. 13, can be adopted.

$$F^n_{i,j}(T_C) - D_{i,j}(T_L, T_M) = \sum_{k=0}^{n} a_k(i,j)(T_C - T_M)^k, \tag{14}$$

where, $T_M$ is the median of the camera temperatures of training sample data and $D_{i,j}(T_L,T_M)$ is the value of the $(i,j)$ pixel at $T_M$.

Let the infrared image of the low-temperature blackbody at the camera temperature $T_{CT}$ be collected to measure the precision of the fitting function (*testing sample data*). The mean squared error (*MSE*) $\delta^n(T_{CT})$ is determined by

$$\delta^n(T_{CT}) = \frac{1}{H \times W} \sum_{i=0}^{H-1} \sum_{j=0}^{W-1} \left[ F^n_{i,j}(T_{CT}) - D_{i,j}(T_L, T_{CT}) \right]^2, \tag{15}$$

where, $H$ ($H$=240) and $W$ ($W$=320) are the height and width of the collected infrared image respectively.

The average MSE of the all testing sample data for the $n^{th}$ degree polynomial $\overline{\delta}^n$ is expressed by the following equation

$$\overline{\delta}^n = \underset{all\ T_{CT}}{avg}\ (\delta^n(T_{CT})). \tag{16}$$

### 4.2 Choice of the degree of the polynomial

Experimental results show that the precision of the fitting function varies with the degree of the polynomial. If the training sample data at $E$ different ambient temperatures are collected, then the degree of the polynomial $n$ ranges from 0 to $E$-1. So, the optimal degree $d$, which causes the minimal average fitting error, can be determined by

$$\overline{\delta}^d = \min_{n \in [0, E-1]} \left( \overline{\delta}^n \right). \tag{17}$$

**Table 1** Average MSE and the coefficients of the 1–6th degree polynomials for (160,120) pixel in the testing sample data.

| Degree | avgMSE | $a_0(i,j)$ | $a_1(i,j)$ | $a_2(i,j)$ | $a_3(i,j)$ | $a_4(i,j)$ | $a_5(i,j)$ | $a_6(i,j)$ |
|---|---|---|---|---|---|---|---|---|
| 1 | 316787.68 | −145.153 | 14.8842 | | | | | |
| 2 | 425.44 | 9.46870 | 52.6880 | 0.131302 | | | | |
| 3 | 317.58 | 1.84802 | 53.4334 | 0.217183 | 0.000291 | | | |
| 4 | 352.56 | 1.99947 | 53.4943 | 0.212692 | −0.000173 | −0.000002 | | |
| 5 | 384.51 | 2.44322 | 53.5023 | 0.205539 | −0.000486 | −0.000001 | 0 | |
| 6 | 439.55 | 10.0535 | 51.4512 | 0.166666 | 0.006227 | −0.000008 | 0 | 0 |

For the purpose, the infrared images of the low-temperature blackbody at 10 different ambient temperatures are collected, seven as the training sample data and the rest as the testing sample data, i.e. $E$=7. From Table 1, it can be seen that, the average MSE of third-degree polynomial reaches minimal value. In addition, the values of $a_5(i,j)$ and $a_6(i,j)$ of the polynomials beyond degree 5 are less than $10^{-6}$. Thus the following third-degree polynomial is adopted.

$$D_{i,j}(T_L, T_C) \approx F^3_{i,j}(T_C) = a_3(i,j)T_C^3 + a_2(i,j)T_C^2 + a_1(i,j)T_C + a_0(i,j). \tag{18}$$

Like Eq. 14, Eq. 18 can be written as

$$D_{i,j}(T_L, T_C) - D_{i,j}(T_L, T_M) \approx \sum_{k=0}^{3} a_k(i,j)(T_C - T_M)^k. \tag{19}$$

Figure 4 depicts the collected pixel values (see "+") and the fitting curves corresponding to Eq. 19, which approximately represents the dependency of $D_{i,j}(T_L,T_C)$ on $T_C$.

Similarly, the pixel value in the infrared image of the high-temperature blackbody is also approximated as a third-degree polynomial of $T_C$.

$$D_{i,j}(T_H, T_C) \approx G^3_{i,j}(T_C) = b_3(i,j)T_C^3 + b_2(i,j)T_C^2 + b_1(i,j)T_C + b_0(i,j), \tag{20}$$

$$D_{i,j}(T_H, T_C) - D_{i,j}(T_H, T_M) \approx \sum_{k=0}^{3} b_k(i,j)(T_C - T_M)^k. \tag{21}$$

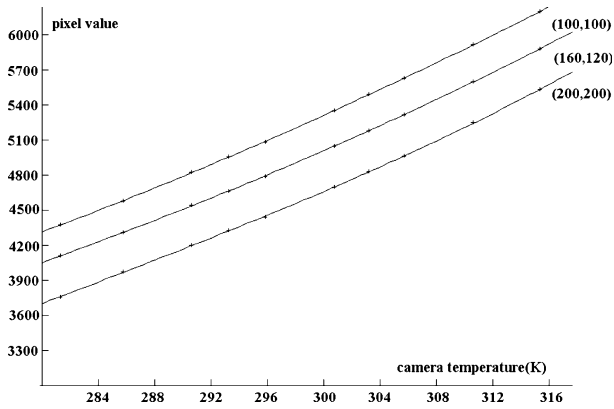


**Fig. 4** Values of the (100, 100), (160,120) and (200,200) pixels in the infrared image of the low temperature blackbody with the camera temperature.

The values of $b_3(i,j)$,…, $b_0(i,j)$ and $a_3(i,j)$,…, $a_0(i,j)$ can be figured out with the values of the $(i,j)$ pixel in the infrared images of the high-temperature and low-temperature blackbodies (*TPC training sample data*) at more than four different camera temperatures, respectively.

### 4.3 Determining the coefficient of the polynomial

Based on the previous discussions, we present a complete description of the building the third-degree polynomial process as follows.

1) At each of the appointed ambient temperature, the TPC training sample data and the corresponding camera temperature are collected.
2) The coefficients of Eqs. 19 and 21 for each pixel are calculated by means of least squares fitting and with the TPC training sample data and their camera temperatures.

### 4.4 Removing the effect of the camera radiance

The process of removing the effect of the camera radiance on infrared image is outlined below.

1) The current camera temperature $T_C$ is collected.
2) The values of each pixel in the infrared images of the low-temperature and high-temperature blackbodies (TPC data) are computed at $T_C$ by using Eqs. 19 and 21, respectively. Then, the gains and offsets are calculated according to

$$Gain_{i,j}(T_C) = \frac{\overline{D(T_H, T_C)} - \overline{D(T_L, T_C)}}{D_{i,j}(T_H, T_C) - D_{i,j}(T_L, T_C)}, \tag{22}$$

$$O_{i,j}(T_C) = D_L - G_{i,j}(T_C) \times D_{i,j}(T_L, T_C), \tag{23}$$

where $Gain_{i,j}(T_C)$ and $O_{i,j}(T_C)$ are gain and offset of the $(i,j)$ pixel, respectively, $\overline{D(T_H, T_C)}$ and $\overline{D(T_L, T_C)}$ are the mean values of $D_{i,j}(T_H,T_C)$ and $D_{i,j}(T_L,T_C)$, respectively.

From Eqs. 22 and 23, Eq. 6 can be rewritten as:

$$D'_{i,j}(T_C) = Gain_{i,j}(T_C) \times D_{i,j}(T_C) + O_{i,j}(T_C). \tag{24}$$

3) The infrared image collected at current camera temperature $T_C$ can be corrected using Eq. 24. As a result, the effect of the camera radiance on the infrared image is removed effectively.

## 5 Experiment

In our experiment, two large area blackbodies referenced as M315X8 [11] are chosen, where the low-temperature blackbody is at 30°C, and the high-temperature blackbody is at 60°C. A temperature chamber is utilized to change the ambient temperature of the camera. The infrared images of the high-temperature and low-temperature blackbodies for six

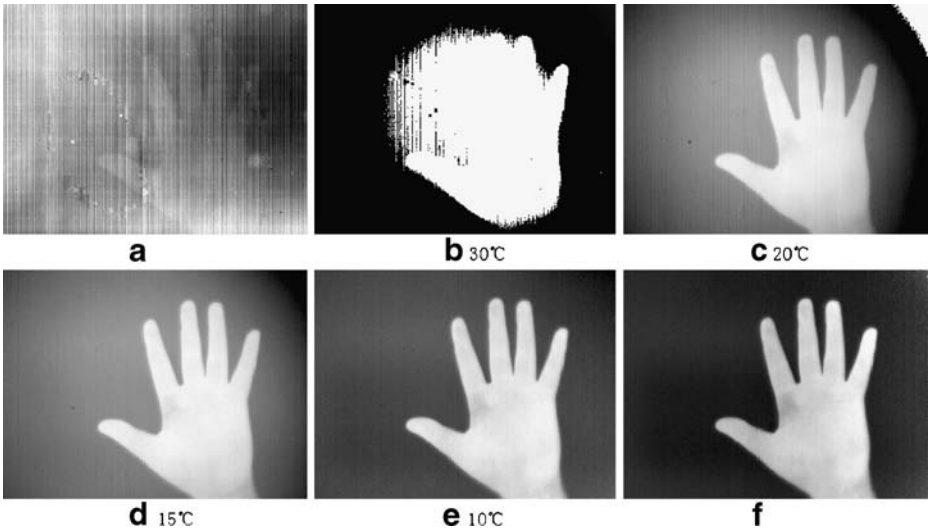


**Fig. 5** Corrected infrared images collected at ambient temperature 8°C (camera temperature 11.25°C) with the TPC data collected at camera temperatures 30, 20, 15 and 10°C and calculated at camera temperature 284.4*K* (11.25°C) (*F*).

different ambient temperatures (5, 10, 15, 20, 30, 40°C) are collected to calculate the coefficients of the Eqs. 19 and 21.

Figure 5 illustrates the corrected infrared images, which is collected at ambient temperature 8°C (camera temperature 11.25°C). *A* is the original infrared image without correction, and *B*, *C*, *D* and *E* are the corrected infrared images with TPC data collected at ambient temperatures 30, 20, 15 and 10°C (camera temperatures 32.562, 22.75, 17.5 and 12.625°C), respectively. *F* denotes the infrared image corrected with the TPC data calculated at camera temperature 284.4*K* (11.25°C) through Eqs. 19 and 21. From Fig. 5, we can see that the closer the camera temperature of the original image is to that of the TPC data, the better the quality of the corrected image is. Among all corrected images, the quality of *F* is the best.

Figure 6 illustrates the corrected infrared images at ambient temperature 26°C (camera temperature 29.69°C). For clarity, the temperature window of the images in Fig. 6 is narrower than that in Fig. 5. In Fig. 6, the left infrared image is corrected by the proposed method and with the TPC data calculated at camera temperature 302.84*K* (29.69°C) through Eqs. 19 and 21. The right one is corrected with the TPC data collected at ambient temperature 30°C (camera temperature 32.562°C). It can be seen that the left one exhibits more details and less pattern noise (vertical line) than the right one.

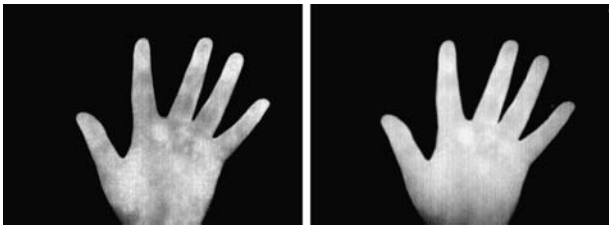

**Fig. 6** Corrected infrared images collected at ambient temperature 26°C (camera temperature 29.69°C) with the TPC data calculated at camera temperature 302.84*K* (29.69°C) (left) and collected at ambient temperature 30°C (camera temperature 32.562°C) (right).

## 6 Conclusions

This paper proposes a new scheme of removing the effect of the camera radiance on the infrared image. Using least squares fitting, the method determines the functions of the pixel values in the infrared images of the high-temperature and low-temperature blackbodies with the camera temperature. With these fitting functions, the two-point-correction data are calculated for a proper camera temperature. Theoretical analysis and experimental results show that the scheme can remove the effect effectively.

**Acknowledgements** The authors are grateful to the anonymous reviewers for their valuable comments and suggestions. This work is supported by Natural Science Foundation of China (10771227), Program for New Century Excellent Talent of Educational Ministry of China (NCET-05-0759), Doctorate Foundation of Educational Ministry of China (20050611001), and Natural Science Foundations of CQ CSTC (2006BB2393, 2006BB2231).

## References

1. N. Horny, "FPA camera standardization," Infrared Physics & Technology **44**, 109–119 (2003)
2. S. D. Dong, X. F. Yang, B. He, and G. J. Liu, "A transplantable compensation scheme for the effect of the radiance from the interior of a camera on the accuracy of Temperature Measurement," International Journal of Infrared and Millimeter Waves **27**, 1517–1528 (2006)
3. B. Fieque, A. Crastes, J. L. Tissot, and S. Tinnes, "320×240 uncooled microbolometer 2D array for radiometric and process control applications," Detectors and Associated Signal Processing **5251**, 114–120 (2004)
4. SOFRADIR, 320×240 LWIR Uncooled microbolometer detector technical specification, *ID ML073-V3/ 28.03.02/NTC Issue 9*, pp. 1–15 (2002)
5. C. G. Kang, "Computer simulation of compensation method for infrared focal plane array," Journal of Beijing Institute of Technology **9**, 330–333 (2000)
6. J. L. Tissot, "IR detection with uncooled sensors," Infrared Physics & Technology **46**, 147–153 (2004)
7. D. A. Scribner, M. R. Kruer, and J. M. Killiany, "Infrared focal-plane array technology," Proceedings of the IEEE **79**, 66–85 (1991)
8. A. F. Milton, F. R. Barone, and M. R. Kruer, "Influence of nonuniformity on infraredfocal plane array performance," Optical Engineering **24**, 855–862 (1985)
9. H. X. Zhou, R. Lai, S. Q. Liu, and G. Jiang, "New improved nonuniformity correction for infrared focal plane arrays," Optics Communications **245**, 49–53 (2005)
10. L. B. Richard and F. J. Douglas, *Numerical Analysis*, 7th ed., pp. 104–107. (Brooks Cole, Pacific Grove, CA, USA, 2000)
11. Mikron, M315X Series: Large Area Precision Blackbody Calibration Sources for Test and Measurement Applications, http://www.mikroninfrared.com/products/ blackbody/m315x.htm